DALTON

Selectivity design using interligand contact: solvent extraction and structures of first-series-transition metal–bis(pyrazol-1-yl)borate complexes

Hisao Kokusen,*[a] Yoshiki Sohrin,[b] Masakazu Matsui,[b] Yasuo Hata[b] and Hiroshi Hasegawa[c]

[a] *Faculty of Education, Department of Chemistry, Tokyo Gakugei University, Koganei, Tokyo 184, Japan*

[b] *Institute for Chemical Research, Kyoto University, Uji, Kyoto 611, Japan*

[c] *Department of Chemistry, Faculty of Science, Kochi University, Akebono-cho, Kochi 780, Japan*

The bis(pyrazol-1-yl)borates $[H_2B(pz)_2]^-$, $[H_2B(pz)(dmpz)_2]^-$ and $[H_2B(dmpz)_2]^-$ (dmpz = 3,5-dimethylpyrazol-1-yl) formed 2:1 complexes with first-series-transition metals, which were extracted into chloroform. The anion $[H_2B(dmpz)_2]^-$ had unique characteristics: (*i*) extraction of the complexes was a slow process for Co^{II} and Ni^{II}; (*ii*) extractability for Ni^{II} was low, and the selectivity pattern did not conform to the Irving–Williams order. The results suggested that its complex formation with small metal ions is kinetically and thermodynamically unfavourable. The crystal structures of $[Ni\{H_2B(pz)(dmpz)_2\}_2]$, $[Ni\{H_2B(dmpz)_2\}_2]$ and $[Co\{H_2B(dmpz)_2\}_2]$ have been determined and compared with those previously reported for $[Ni\{H_2B(pz)_2\}_2]$ and $[Co\{H_2B(pz)_2\}_2]$. The complexes are similar in that the geometry at Ni^{II} is square planar and that at Co^{II} is tetrahedral. However, $[Co\{H_2B(dmpz)_2\}_2]$ contains the highest interligand contact and is highly strained. This contact is the origin of the unusual selectivity of $[H_2B(dmpz)_2]^-$.

The stability of co-ordination compounds of first-series-transition metals usually increases in the order $Mn^{II} < Fe^{II} < Co^{II} < Ni^{II} < Cu^{II} > Zn^{II}$, *i.e.* the Irving–Williams series which is mainly dominated by electronic factors.[1–3] Selectivity for metal ions in solvent extraction of chelate complexes ordinarily follows this series.[4] To design a new and unique selectivity for metal ions it seems most practical to utilize steric factors.

We have been investigating the solvent extraction of metal ions using poly(pyrazol-1-yl)borates, $[H_nB(pz)_{4-n}]^-$ (n = 0–2), which have a unique structure and selectivity.[5] Here, we report on the extraction of first-series-transition metals with bis(pyrazol-1-yl)borates. Dihydrobis(pyrazol-1-yl)borate, $[H_2B(pz)_2]^-$ and bis(3,5-dimethylpyrazol-1-yl)dihydroborate, $[H_2B(dmpz)_2]^-$, were first reported by Trofimenko[6] and (3,5-dimethylpyrazol-1-yl)dihydro(pyrazol-1-yl)borate, $[H_2B(pz)(dmpz)]^-$, was reported by Frauendorfer and Agrifoglio.[7] They consist of a tetrahedral boron atom bonded to pyrazolyl groups, and act as bidentate ligands forming a six-membered chelated ring with a boat conformation.[8] The prime objective of this study was to determine how a methyl group at the 3 position of the pyrazolyl ring changes the selectivity of the anion for metal ions.

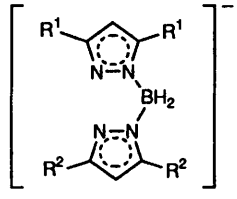

	R^1	R^2
$[H_2B(pz)_2]^-$	H	H
$[H_2B(pz)(dmpz)]^-$	H	Me
$[H_2B(dmpz)_2]^-$	Me	Me

Results

Protonation and partition constants of bis(pyrazolyl)borates

Bis(pyrazol-1-yl)borates are diprotic bases. The protonation constants are defined in equations (1) and (2) where brackets

$$K_{HA} = [HA]/[H^+][A^-] \quad (1)$$

$$K_{H_2A} = [H_2A^+]/[H^+][HA] \quad (2)$$

represent the molar concentration in aqueous solution and A^- is a bis(pyrazol-1-yl)borate anion. From pH titrations, $[H_2B(pz)_2]^-$, log K_{HA} and log K_{H_2A} were found to be 8.70 and 4.99, respectively for $[H_2B(pz)_2]^-$, 9.05 and 6.04 for $[H_2B(pz)(dmpz)]^-$ and 9.80 and 7.23 for $[H_2B(dmpz)_2]^-$.[5a]

The partition constant of a bis(pyrazol-1-yl)borate is defined in equation (3) where the subscript o denotes the species in the

$$P_{HA} = [HA]_o/[HA] \quad (3)$$

organic phase, and the distribution ratio of the anion between the aqueous and chloroform phases is defined as in equation (4). Plots of log D_{HA} as a function of pH were analysed by a non-

$$D_{HA} = [HA]_o/([H_2A^+] + [HA] + [A^-]) \quad (4)$$

linear least-squares method, and partition and protonation constants obtained. The bis(pyrazol-1-yl)borates are hydrolysed in water to pyrazole and boric acid. In the distribution experiments the borate concentrations in both phases decreased with increasing shaking time. The decomposition rate of $[H_2B(pz)_2]^-$ was highest around pH 5–9, that of $[H_2B(pz)(dmpz)]^-$ was almost independent of pH, and that of $[H_2B(dmpz)_2]^-$ was lowest between pH 7 and 10 at which the concentration in the aqueous phase was the lowest. It increased in the order $[H_2B(pz)_2]^- < [H_2B(pz)(dmpz)]^- < [H_2B(dmpz)_2]^-$. To remove the influence of hydrolysis, log $[HA]_o$ was plotted against t, the value at $t = 0$ was obtained by extrapolation and used for plots of D_{HA} *vs.* pH. The log P_{HA} for partition between the chloroform and aqueous phases was 0.20 for $H[H_2B(pz)_2]$, 0.72 for $H[H_2B(pz)(dmpz)]$ and 1.60 for $H[H_2B(dmpz)_2]$. Protonation constants of bis(pyrazol-1-yl)-

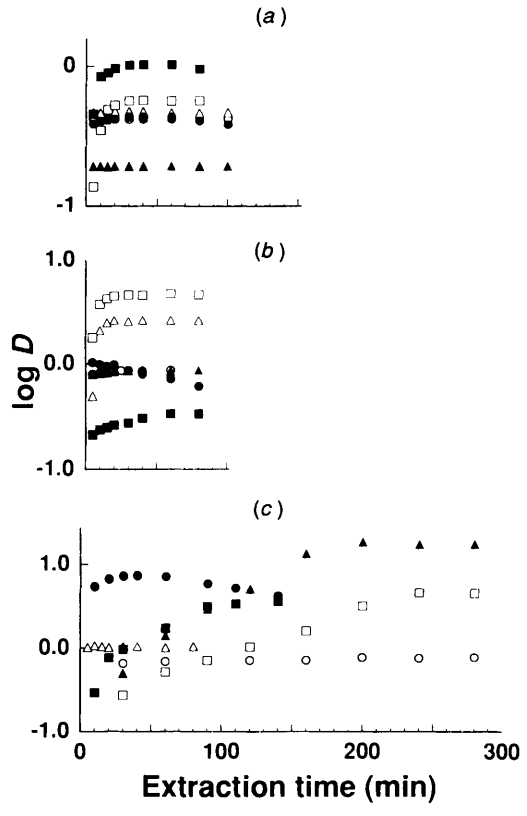

Fig. 1 Plots of log D as a function of extraction time with $[H_2B(pz)_2]^-$ (*a*), $[H_2B(pz)(dmpz)]^-$ (*b*) and $[H_2B(dmpz)_2]^-$ (*c*). ○, Cu^{II}; △, Zn^{II}; □, Ni^{II}; ▲, Co^{II}; ■, Fe^{II}; ●, Mn^{II}

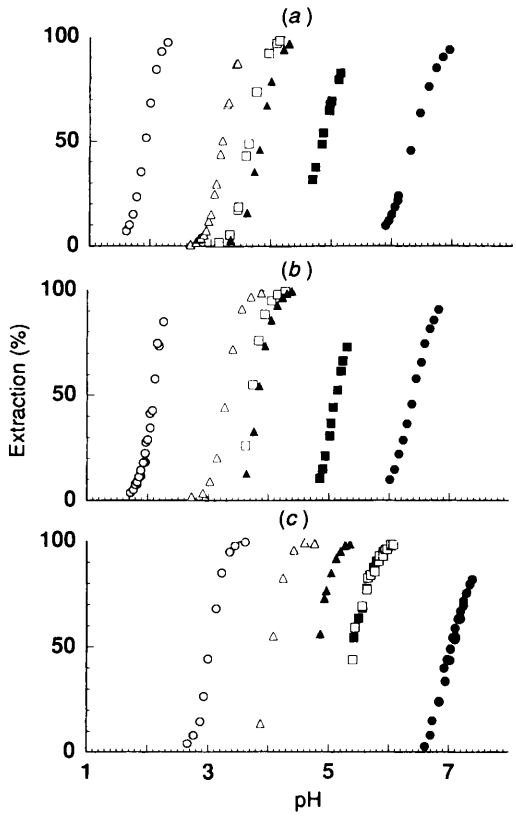

Fig. 2 Plots of the extraction ratio as a function of pH. The initial c_{HA} was 1×10^{-2} mol dm^{-3} for $[H_2B(pz)_2]^-$ (*a*), $[H_2B(pz)(dmpz)]^-$ (*b*) and $[H_2B(dmpz)_2]^-$ (*c*). Metal ions as in Fig. 1

borates determined by the distribution method agreed with those obtained by the titration method. Hydrolysis did not significantly influence the titrations of the borates since the latter were complete within 30 min.

Time dependence of the extractions of transition metals

The distribution ratios, D, of transition-metal ions, as defined in equation (5) where c_M signifies the analytical molar

$$D = c_{M,o}/c_M \quad (5)$$

concentration of the metal ion, were plotted as a function of extraction time in Fig. 1. The log D values in the $[H_2B(pz)_2]^-$ and $[H_2B(pz)(dmpz)]^-$ systems reached maxima within 60 min of shaking. However, prolonged shaking was needed to attain the maximum log D for $[H_2B(dmpz)_2]^-$: 120 min for Fe^{II} and 240 min for Co^{II} and Ni^{II}.

Equilibrium analysis of transition metals

The extraction ratios of the transition metals with $[H_2B(pz)_2]^-$, $[H_2B(pz)(dmpz)]^-$ and $[H_2B(dmpz)_2]^-$ are plotted as a function of pH in Fig. 2. The shaking period was 60 min for $[H_2B(pz)_2]^-$ and $[H_2B(pz)(dmpz)]^-$ except for 15 min in the Mn^{II}–$[H_2B(pz)(dmpz)]^-$ system. In the $[H_2B(dmpz)_2]^-$ system the phases were shaken for 40 min for Mn^{II}, 60 min for Cu^{II} and Zn^{II}, 120 min for Fe^{II} and 240 min for Co^{II} and Ni^{II}. The extraction ratio was independent of the metal ion concentration between 2×10^{-5} and 3×10^{-4} mol dm^{-3}. The overall extraction equilibrium and extraction constant (K_{ex}) of a transition-metal ion (M^{2+}) can be expressed by equations (6)–(8).

$$M^{2+} + 2HA \rightleftharpoons MA_{2,o} + 2H^+ \quad (6)$$

$$K_{ex} = [MA_2]_o[H^+]^2/[M^{2+}][HA]^2 \quad (7)$$

$$\log K_{ex} = \log D - 2pH - 2 \log [HA] \quad (8)$$

To analyse the extraction data graphically, the acid protonation and distribution of the bis(pyrazol-1-yl)borates must be taken into consideration. The concentration [HA] is expressed as in equation (9) where c_{HA} means the total anal-

$$[HA] = c_{HA}/\{P_{HA} + (1/K_{HA}[H^+]) + 1 + K_{H_2A}[H^+]\} \quad (9)$$

ytical concentration of the bis(pyrazol-1-yl)borate. Substitution of equation (7) into (8) and rearrangement results in expressions (10) and (11). Plots of log D − 2(log c_{HA} − α) on pH

$$\log D = \log K_{ex} + 2pH + 2 \log c_{HA} - 2\alpha \quad (10)$$

$$\alpha = \log\{P_{HA} + (1/K_{HA}[H^+]) + 1 + K_{H_2A}[H^+]\} \quad (11)$$

and of log D − 2(pH − α) on log c_{HA} were made for all the borates and metal ions. All were linear with slopes very close to 2. These results confirmed the validity of equations (6) and (10). Dimerization of the borates was negligible under these experimental conditions. The log K_{ex} values, obtained from the plots of log D − 2(log c_{HA} − α) *vs.* pH by a linear least-squares fit, are listed in Table 1.

In the $[H_2B(dmpz)_2]^-$ system, c_{HA} decreased to 20% of its initial value after 240 min of shaking. The c_{HA} values have been corrected for the hydrolysis effect in the data shown in Table 1.

The log K_{ex} values for $[H_2B(pz)_2]^-$ are somewhat different from those in our previous report.[5a] This may be due to a difference in the ion strength in the aqueous phases.

Synthesis of complexes

Complexes with two bis(pyrazol-1-yl)borates co-ordinated to Ni^{II} and Co^{II} were produced according to equation (12). They

$$M^{2+} + 2A^- \rightleftharpoons MA_2 \quad (12)$$

Table 1 Extraction constants (log K_{ex}) of first-series-transition metals with bis(pyrazol-1-yl) borates

Metal ion	$[H_2B(pz)_2]^-$	$[H_2B(pz)(dmpz)]^-$	$[H_2B(dmpz)_2]^-$
Mn^{II}	−7.16	−7.83	−6.96
Fe^{II}	−3.96	−3.82	−2.64
Co^{II}	−1.09	0.86	0.59
Ni^{II}	−0.46	1.35	−1.60
Cu^{II}	6.21	7.84	6.66
Zn^{II}	1.15	3.02	2.53

were obtained as precipitates and were soluble in chloroform, benzene and dichloromethane. All were stable in air.

Structures of nickel(II) complexes of bis(pyrazol-1-yl)borates

The structure of $[Ni\{H_2B(pz)_2\}_2]$ **1** was reported by Echols and Dennis.[9] Figs. 3 and 4 show ORTEP[10] drawings of $[Ni\{H_2B(pz)(dmpz)\}_2]$ **2** and $[Ni\{H_2B(dmpz)_2\}_2]$ **3**, respectively. Selected bond distances and the angles are given in Tables 2 and 3, respectively. These complexes have a nickel atom at a centre of inversion. All the ligands in **1–3** are bidentate, and the geometry about the nickel atom is square planar. The mean dimensions of **1–3** are summarized and compared in Table 5.

Structures of cobalt(II) complexes of bis(pyrazol-1-yl)borates

The structure of $[Co\{H_2B(pz)_2\}_2]$ **4** has been reported by Guggenberger *et al.*[11] Fig. 5 shows an ORTEP drawing of $[Co\{H_2B(dmpz)_2\}_2]$ **5**. Selected bond distances and angles are listed in Table 4.

The cobalt atom is on a two-fold axis.

Both the ligands in **4** and **5** are bidentate, forming four-co-ordinated, monomeric structures, and the geometry about the cobalt atom is distorted tetrahedral. Mean dimensions of **4** and **5** are compared in Table 5.

Discussion

Unusual features of $[H_2B(dmpz)_2]^-$ in the extraction of first-series-transition metals

With $[H_2B(pz)_2]^-$, $[H_2B(pz)(dmpz)]^-$ and $[H_2B(dmpz)_2]^-$, all the first-series-transition-metal ions formed MA_2 complexes and were quantitatively extracted into the chloroform phase. However, $[H_2B(dmpz)_2]^-$ was different in that prolonged shaking was required to extract Ni^{II} and Co^{II} (Fig. 1). The results suggested that the formation of $[H_2B(dmpz)_2]^-$ complexes with small metal ions is a slow process. The change in log K_{ex} in the first transition series is shown in Fig. 6. Although the trend for $[H_2B(pz)_2]^-$ and $[H_2B(pz)(dmpz)]^-$ obeys the Irving–Williams order, that of $[H_2B(dmpz)_2]^-$ is distinct, log K_{ex} for Ni^{II} being significantly low. As a result, the selectivity of $[H_2B(dmpz)_2]^-$ for Cu^{II} over Ni^{II} was improved by 40-fold compared with that of $[H_2B(pz)_2]^-$.

The K_{ex} may be represented as in equation (13) where P_{MA_2} is

$$K_{ex} = P_{MA_2}\beta_{MA_2}/K_{HA}^2 \qquad (13)$$

the partition constant and β_{MA_2} the stability constant of the complex. We did not determine P_{MA_2} because its values were very high. It should not change irregularly at Ni^{II}. It is very likely that the tendency of K_{ex} is controlled by the change in β_{MA_2}. Similar results were obtained by Jezorek and McCurdy.[12] They determined the enthalpy (ΔH) of precipitation of Co^{II}, Ni^{II}, Cu^{II} and Zn^{II} by $[H_2B(pz)_2]^-$ and $[H_2B(mpz)_2]^-$ (mpz = 3-methylpyrazol-1-yl) in aqueous media. The increase in ΔH was much larger for Ni^{II} than that for Cu^{II} when the ligand was changed from $[H_2B(pz)_2]^-$ to $[H_2B(mpz)_2]^-$.

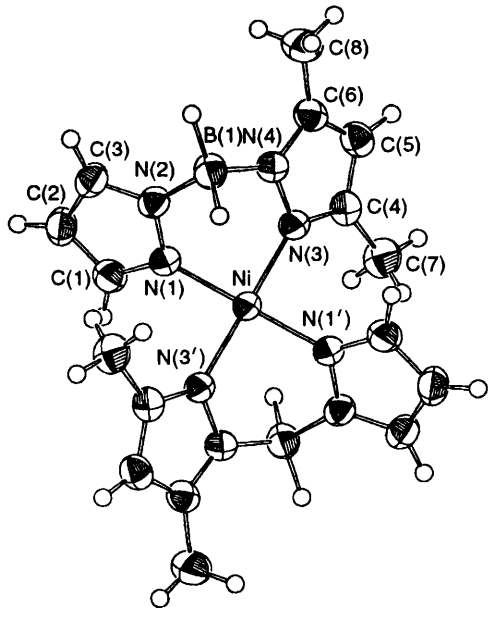

Fig. 3 An ORTEP view of $[Ni\{H_2B(pz)(dmpz)\}_2]$ **2** (50% probability ellipsoids)

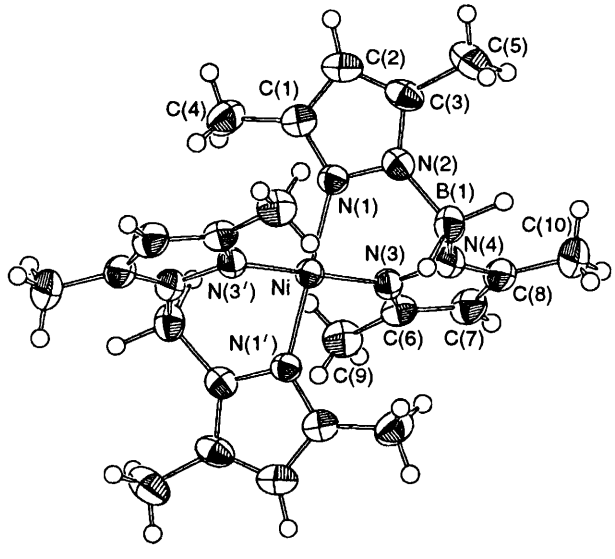

Fig. 4 An ORTEP view of $[Ni\{H_2B(dmpz)_2\}_2]$ **3** (50% probability ellipsoids)

Interligand contact

The unusual features of $[H_2B(dmpz)_2]^-$ complexes are connected with small metal ions. A steric effect of the methyl groups is believed to be responsible. It has been found in MA_2 complexes of bis(pyrazol-1-yl)borates that the geometry is tetrahedral for Mn^{II}, Fe^{II}, Co^{II} and Zn^{II} and square planar for Ni^{II} and Cu^{II};[8a] Co^{II} and Ni^{II} are the smallest ions in each geometry.[13] To examine the steric effects, $[Ni\{H_2B(pz)(dmpz)\}_2]$ **2**, $[Ni\{H_2B(dmpz)_2\}_2]$ **3** and $[Co\{H_2B(dmpz)_2\}_2]$ **5** were synthesized, and their structures determined by X-ray crystallography and compared with those of $[Ni\{H_2B(pz)_2\}_2]$ **1**[9] and $[Co\{H_2B(pz)_2\}_2]$ **4**[11] (Table 5). The geometry in **1–3** is square planar. The Ni–N bond lengths are identical, while the bite sizes (N ··· N) and bite angles (N–M–N) slightly decrease with increasing number of methyl groups. The interligand distance between the carbon atoms at the 3 position of the pyrazolyl rings (3C ··· 3C) is only 3.30 Å for **1**. When the 3-methyl group is introduced into the structure of **1** the

Table 2 Selected bond distances (Å) and angles (°) for [Ni{H_2B(pz)-(dmpz)}$_2$] **2**

Ni–N(1)	1.883(3)	Ni–N(3)	1.894(2)
N(1)–N(2)	1.353(3)	N(2)–B(1)	1.553(4)
N(3)–N(4)	1.375(3)	N(4)–B(1)	1.548(4)
N(1)–Ni–N(1′)	180.0	N(1)–Ni–N(3)	89.82(10)
N(1)–Ni–N(3′)	90.18(10)	Ni–N(1)–N(2)	119.4(2)
N(1)–N(2)–B(1)	119.3(2)	Ni–N(3)–N(4)	119.9(2)
N(3)–N(4)–B(1)	117.6(2)	N(2)–B(1)–N(4)	105.1(2)

Table 3 Selected bond distances (Å) and angles (°) for [Ni{H_2B-(dmpz)$_2$}$_2$] **3**

Ni–N(1)	1.893(2)	Ni–N(3)	1.889(2)
N(1)–N(2)	1.357(3)	N(2)–B(1)	1.556(4)
N(3)–N(4)	1.365(3)	N(4)–B(1)	1.551(5)
N(1)–Ni–N(1′)	180.0	N(1)–Ni–N(3)	89.11(9)
N(1)–Ni–N(3′)	90.89(9)	Ni–N(1)–N(2)	118.3(2)
N(1)–N(2)–B(1)	117.6(2)	Ni–N(3)–N(4)	117.9(2)
N(3)–N(4)–B(1)	117.9(2)	N(2)–B(1)–N(4)	105.0(3)

Table 4 Selected bond distances (Å) and angles (°) for [Co{H_2B-(dmpz)$_2$}$_2$] **5**

Co–N(1)	1.991(3)	Co–N(3)	1.992(3)
N(1)–N(2)	1.362(4)	N(2)–B(1)	1.552(6)
N(3)–N(4)	1.373(4)	N(4)–B(1)	1.548(6)
N(1)–Co–N(1′)	138.8(2)	N(1)–Co–N(3)	97.8(1)
N(1)–Co–N(3′)	106.0(1)	N(3)–Co–N(3′)	108.3(2)
Co–N(1)–N(2)	119.0(2)	N(1)–N(2)–B(1)	118.6(3)
Co–N(3)–N(4)	119.8(2)	N(3)–N(4)–B(1)	117.9(3)
N(2)–B(1)–N(4)	109.9(3)		

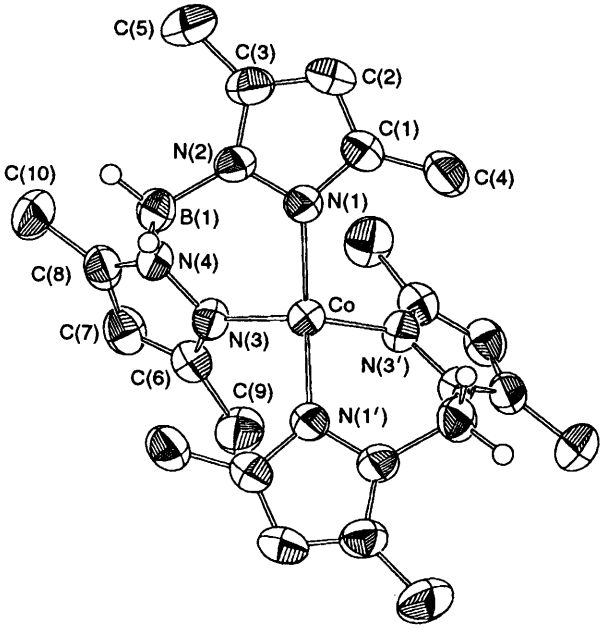

Fig. 5 An ORTEP view of [Co{H_2B(dmpz)$_2$}$_2$] **5** (50% probability ellipsoids). Hydrogen atoms are omitted for clarity

interligand distances, such as 3Me···3Me and 3C···3Me, are rather short judging from the van der Waals radii of the methyl group (2.0 Å) and the sp^2 carbon atom (1.77 Å).[14] To avoid interligand contacts, [H_2B(pz)(dmpz)]$^-$ and [H_2B(dmpz)$_2$]$^-$ assume a different conformation from that of [H_2B(pz)$_2$]$^-$. The distance between Ni^{II} and the boron atom (M···B), the M–N–N angle and the dihedral angle a

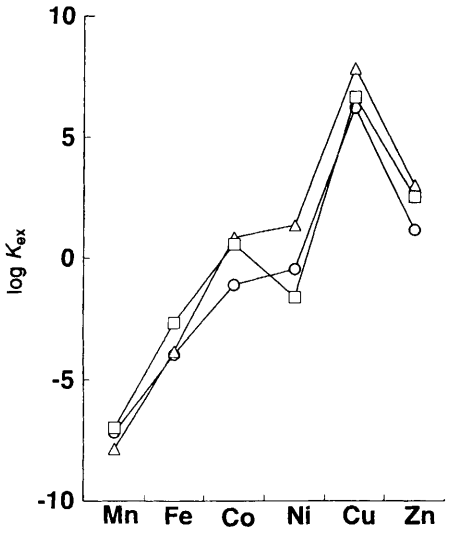

Fig. 6 Selectivity patterns in the extraction of first-series-transition-metal ions with bis(pyrazolyl)borates. ○, [H_2B(pz)$_2$]$^-$; △, [H_2B-(pz)(dmpz)]$^-$; □, [H_2B(dmpz)$_2$]$^-$

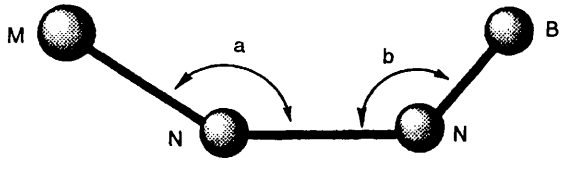

(M–N···N–N) decrease as the number of 3-methyl groups increases. This means that the boat of the chelate ring deepens using [H_2B(pz)(dmpz)]$^-$ and [H_2B(dmpz)$_2$]$^-$. However, the conformation change is not sufficient to release the interligand contacts for **3**. The arrows in Fig. 7 show severe steric contacts. Compound **3** contains at least six severe interligand contacts: 3Me···3Me 4.00 and 3C···3Me 3.52–3.47 Å. Thus, complex **3** is highly strained, which is responsible for the diminished stability and selectivity of [H_2B(dmpz)$_2$]$^-$ for Ni^{II}.

The introduction of 3-methyl groups also changes the ligand conformation in the tetrahedral cobalt(II) complex **5**. The M···B distance and the dihedral angle a were larger than those of **4**. The tetrahedron was more distorted. The interligand N···N distance was 3.18–3.73 Å for **5**, whereas it was 3.17–3.47 Å for **4**.[11] The interligand N–M–N angle was 106.0–138.8° for **5**, 106.7–122.1° for **4**.[11] The conformation change resulted in an increase in the smallest 3C···3C distance from 3.68 Å in **4** to 3.97 Å in **5**. The remaining severe interligand contact in **5** was a 3Me···3Me distance (3.90 Å, Fig. 7). Since the van der Waals strain in **5** is much lower than that in **3**, the selectivity of [H_2B(dmpz)$_2$]$^-$ does not obey the Irving–Williams order. The interligand contact becomes more serious for a smaller metal ion, such as Be^{2+}: the ionic radius is 72 pm for Co^{II} and 41 pm for Be^{2+} in tetrahedral co-ordination.[13] Actually, although [HB(pz)$_3$]$^-$ forms a tetrahedral MA_2 complex with Be^{2+}, in which the ligand is bidentate, [HB(dmpz)$_3$]$^-$ cannot form such a complex because of the steric effects of the 3-methyl group.[5c]

We speculate that the slow extraction with [H_2B(dmpz)$_2$]$^-$ is also affected by the interligand contact. The rate-determination step for complex formation in this system probably does not follow the Eigen mechanism.[15] The rate must be determined not by the dissociation of co-ordinated water molecules but by co-ordination of the second ligand.

In conclusion, bis(pyrazol-1-yl)borates are flexible and reduce interligand contacts through a conformational change. However, this is not so effective for very small ions. The interligand contact can be used to give an unprecedented feature to bis(pyrazol-1-yl)borates.

Table 5 Mean dimensions (Å or °) of $[Ni\{H_2B(pz)_2\}_2]$ **1**, **2**, **3**, $[Co\{H_2B(pz)_2\}_2]$ **4** and **5**

	1[a]	2	3	4[b]	5
M–N	1.90(1)	1.89(1)	1.89(1)	1.97(2)	1.99(1)
N · · · N[c]	2.69(1)	2.67(1)	2.65(1)	2.95(4)	3.00(1)
M · · · B	3.14(1)	3.05(1)	2.99(1)	3.01(1)	3.14(1)
3C · · · 3C[d]	3.30(1)	3.39(1)	3.50(1)	3.68(1)	3.97(1)
N–M–N[e]	90.8(0.1)	89.8(0.1)	89.1(0.1)	97.0(1.0)	97.8(0.1)
M–N–N	122.0(0.1)	119.6(0.3)	118.1(0.2)	117.0(1.2)	119.4(0.4)
N–N–B	119.1(0.2)	118.5(0.8)	117.8(0.2)	117.6(1.7)	118.3(0.4)
Angle a[f]	148.2(1.0)	140.8(0.8)	137.0(0.8)	150.1(3.0)	162.7(0.7)
Angle b[g]	132.6(1.2)	133.5(0.9)	132.6(0.8)	126.9(2.6)	126.3(0.8)

[a] Data taken from ref. 9. [b] Data taken from ref. 11. [c] Intraligand distance of donor atoms. [d] Shortest interligand distance between carbon atoms at the 3 position of the pyrazole rings. [e] In chelate rings. [f] Dihedral angle M–N · · · N–N. [g] Dihedral angle B–N · · · N–N.

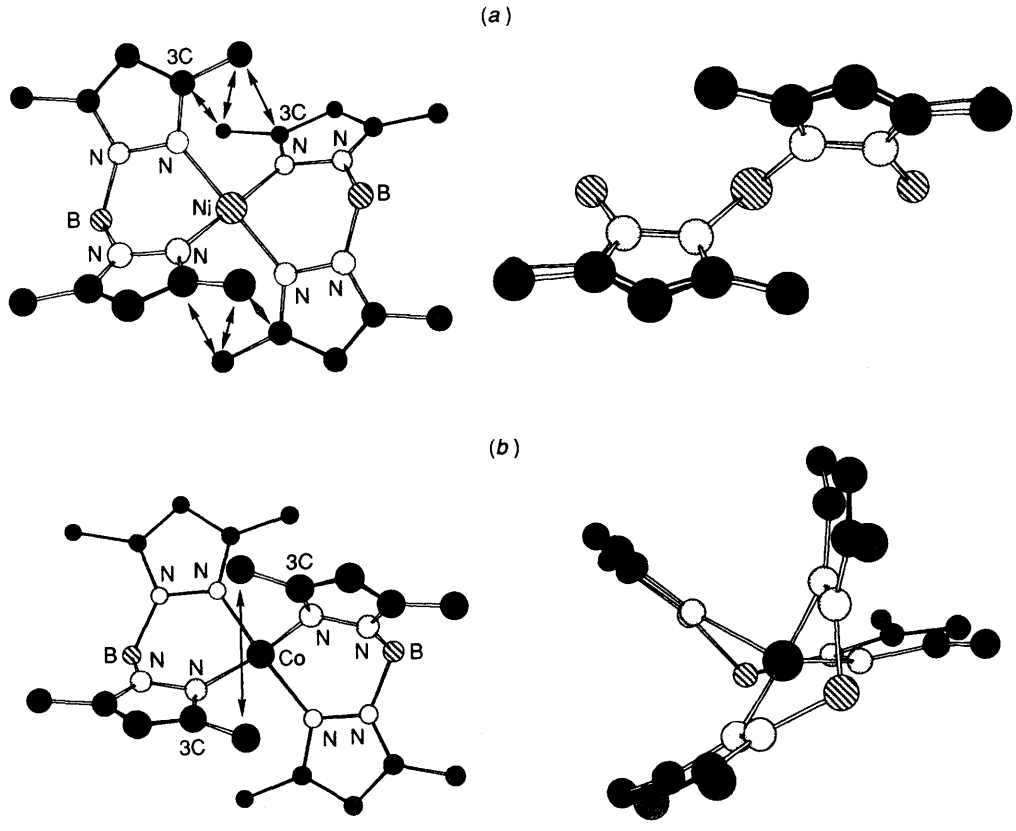

Fig. 7 Crystal structures of (*a*) $[Ni\{H_2B(dmpz)_2\}_2]$ **3** and (*b*) $[Co\{H_2B(dmpz)_2\}_2]$ **5** showing severe steric contacts (arrows)

Experimental

Reagents and apparatus

The salts $K[H_2B(pz)_2]$ and $K[H_2B(dmpz)_2]$ were synthesized according to the method of Trofimenko.[6] The latter was recrystallized from toluene. For further purification, it was dissolved in water to which acetic acid was added until a white precipitate of $H[H_2B(dmpz)_2]$ no longer formed (pH 8). The precipitate was filtered off and dried *in vacuo* (Found: C, 58.90; H, 8.40; N, 27.45. $C_{10}H_{17}BN_4$ requires C, 58.85; H, 8.40; N, 27.45%). The acid $H[H_2B(pz)(dmpz)]$ was synthesized according to the method of Frauendorfer and Agrifoglio.[7] All other chemicals were reagent-grade materials, and distilled water was used throughout.

The pH was measured using a Hitachi-Horiba F-13 pH meter equipped with a glass electrode. The metal-ion concentration was determined using a Seiko SAS760 atomic absorption spectrometer, and the ligand concentration with a Seiko SPS 1200A inductively coupled argon-plasma spectrometer.

Protonation and distribution of bis(pyrazolyl)borates

Protonation constants were determined by potentiometric titration. An aqueous solution (100 cm^3) containing 5×10^{-3} mol dm^{-3} $K[H_2B(pz)_2]$, $H[H_2B(pz)(dmpz)]$ or $H[H_2B(dmpz)_2]$, 1×10^{-2} mol dm^{-3} sodium hydroxide and 0.1 mol dm^{-3} potassium chloride was titrated with 0.1 mol dm^{-3} hydrochloric acid containing 0.1 mol dm^{-3} potassium chloride in a stream of argon at 25.0 ± 0.1 °C.

The distribution was studied in a centrifuge tube (30 cm^3). For $[H_2B(pz)_2]^-$, an aliquot of chloroform (10 cm^3) was equilibrated with an equal volume of an aqueous phase containing 1×10^{-2} mol dm^{-3} $K[H_2B(pz)_2]$ and 0.1 mol dm^{-3} potassium chloride buffered with 2×10^{-2} mol dm^{-3} sodium acetate, 2-(morpholinoethanesulfonic acid), 2-acetamido-2-aminoethanesulfonic acid, 3-morpholinopropanesulfonic acid, *N*-tris(hydroxymethyl)methyl-3-aminopropanesulfonic acid, 2-(cyclohexylamino)ethanesulfonic acid or 3-cyclohexylamino-propanesulfonic acid at 25 ± 1 °C. For $[H_2B(pz)(dmpz)]^-$ and $[H_2B(dmpz)_2]^-$ the free acids were initially dissolved in

Table 6 Crystallographic data for complexes **2**, **3** and **5**

	2	**3**	**5**
Formula	$C_{16}H_{24}B_2N_8Ni$	$C_{20}H_{32}B_2N_8Ni$	$C_{20}H_{32}B_2CoN_8$
M	408.74	464.85	465.08
Crystal size/mm	0.20 × 0.10 × 0.30	0.25 × 0.10 × 0.25	0.30 × 0.10 × 0.30
Crystal system	Monoclinic	Monoclinic	Monoclinic
Space group	$P2_1/c$ (no. 14)	$P2_1/n$ (no. 14)	$C2/c$ (no. 15)
a/Å	7.761(1)	7.739(2)	8.429(3)
b/Å	9.816(2)	17.607(1)	14.371(2)
c/Å	12.937(1)	8.596(1)	19.978(1)
β/°	91.38(1)	95.46(2)	91.23(1)
U/Å^3	985.3(2)	1 166.0(3)	2 419.4(7)
Z	2	2	4
D_c/g cm^{-3}	1.378	1.324	1.277
$F(000)$	428.00	492.00	980.00
μ(Cu-Kα)/cm^{-1}	15.59	13.80	57.37
Measured reflections	1581	1762	1833
Unique reflections (R_{int})	1453 (0.014)	1639 (0.066)	1683 (0.013)
Observed reflections [$I > 3\sigma(I)$]	1213	1429	1496
R, R'*	0.042, 0.068	0.044, 0.069	0.051, 0.069
Goodness of fit	1.94	1.97	1.87

* $R = \Sigma||F_o| - |F_c||/\Sigma|F_o|$; $R' = [\Sigma w(|F_o| - |F_c|)^2/\Sigma w F_o^2]^{\frac{1}{2}}$.

chloroform. After the two phases had been separated by centrifugation the pH of the aqueous phase was measured. The ligand concentration in the aqueous phase was determined from the boron content using the SPS 12000A spectrometer. The concentration in the organic phase was measured after back extraction into 0.2 mol dm^{-3} potassium hydroxide and shaking with a small amount of anhydrous sodium sulfate.

Distribution of the metal chelates

Transition-metal ions were extracted in a manner similar to that of the borates. The borate concentration was 1 × 10^{-2} mol dm^{-3} in chloroform for $H[H_2B(pz)(dmpz)]$ or $H[H_2B(dmpz)_2]$, and the same in aqueous solution for $K[H_2B(pz)_2]$. An aliquot of chloroform (10 cm^3) and an equal volume of an aqueous phase containing a transition-metal ion (1 × 10^{-4} mol dm^{-3}), potassium chloride (0.1 mol dm^{-3}) and buffer (2 × 10^{-2} mol dm^{-3}) were shaken at 25 ± 1 °C. After the two phases had separated the pH and metal concentration in the aqueous phase were determined. The metal concentration in the organic phase was determined after back extraction into 0.1 or 1.0 mol dm^{-3} nitric acid.

Syntheses

Bis[(3,5-dimethylpyrazol-1-yl)dihydro(pyrazol-1-yl)borato]-nickel 2. A 100 cm^3 volume of 0.1 mol dm^{-3} potassium hydroxide containing $H[H_2B(pz)(dmpz)]$ (1.760 g, 10 mmol) was added to an acidic aqueous solution (100 cm^3) of $NiCl_2·6H_2O$ (1.188 g, 5 mmol). Potassium hydroxide solution (0.2 mol dm^{-3}) was added with mixing, until a precipitate no longer formed (pH 5). After 1 h the orange precipitate was filtered off and washed with distilled water, cold methanol and cold heptane. Orange crystals for X-ray crystallography were obtained by recrystallization from a mixture of dichloromethane and heptane (68%) (Found: C, 47.05; H, 5.90; N, 27.40. $C_{16}H_{24}B_2N_8Ni$ requires C, 47.02; H, 5.90; N, 27.45%).

Bis[bis(3,5-dimethylpyrazol-1-yl)dihydroborato]nickel 3. A 20 cm^3 volume of a 0.05 mol dm^{-3} sodium hydroxide solution of $H[H_2B(dmpz)_2]$ (0.41 g, 2 mmol) was added to an acidic aqueous solution (20 cm^3) of $NiSO_4·6H_2O$ (0.26 g, 1 mmol). Sodium hydroxide (0.1 mol dm^{-3}) was added with mixing, until a precipitate no longer formed (pH 6.5). After 75 min the orange precipitate was filtered off and washed with water and methanol. Orange crystals for X-ray crystallography were obtained by recrystallization from dichloromethane (58.1%) (Found: C, 51.50; H, 7.00; N, 24.20. $C_{20}H_{32}B_2N_8Ni$ requires C, 51.65; H, 6.95; N, 24.10%).

Bis[bis(3,5-dimethylpyrazol-1-yl)dihydroborato]cobalt 5. A 20 cm^3 volume of a sodium hydroxide solution of $H[H_2B(dmpz)_2]$ (0.38 g, 1.9 mmol) was added to an aqueous solution (20 cm^3) of $CoCl_2·6H_2O$ (0.23 g, 0.95 mmol). Sodium hydroxide (0.1 mol dm^{-3}) was added with mixing, until a precipitate no longer formed (pH 5.5). After 20 min the purple precipitate was filtered off and washed with water and methanol. Purple crystals for X-ray crystallography were obtained by recrystallization from chloroform–cyclohexane (1:1) (Found: C, 50.50; H, 7.00; N, 23.95. $C_{20}H_{32}B_2CoN_8$ requires C, 51.65; H, 6.95; N, 24.10%).

Crystal structure determinations

Crystallographic data for complexes **2**, **3** and **5** are summarized in Table 6. Crystals were mounted on fine glass fibres with epoxy cement. The lattice parameters and intensity data were measured on a Rigaku AFC7R diffractometer with nickel-filtered Cu-K_α radiation (λ = 1.547 18 Å) at 20 ± 1 °C. The ω–2θ scan technique ($3 \leqslant 2\theta \leqslant 120°$) was used. An empirical absorption correction using the program DIFABS[16] was applied. The data were corrected for Lorentz and polarization effects. A correction for secondary extinction was applied for **3** and **5**. The structures were solved by direct[17] or heavy-atom Patterson methods,[18] expanded using Fourier techniques,[18] and refined by full-matrix least squares. The non-hydrogen atoms were refined anisotropically. Hydrogen atoms were generated by calculation and fixed. All calculations were performed using the TEXSAN package.[19] The final positional parameters for non-hydrogen atoms are listed in Tables 7, 8 and 9 for **2**, **3** and **5**, respectively.

Complete atomic coordinates, thermal parameters and bond lengths and angles, have been deposited at the Cambridge Crystallographic Data Centre. See Instructions for Authors, *J. Chem. Soc., Dalton Trans.*, 1996, Issue 1.

Acknowledgements

We thank Professor Kenju Watanabe and Akira Saitoh for helpful discussion. This research was supported by Grants-in-Aid (Nos. 06740556 and 06740558) from the Ministry of Education, Science and Culture, Japan.

Table 7 Fractional atomic coordinates for complex **2**

Atom	*x*	*y*	*z*
Ni	0.5	0.0	0.0
N(1)	0.4209(3)	0.0261(2)	0.1351(2)
N(2)	0.3405(3)	0.1439(2)	0.1589(2)
N(3)	0.2846(3)	0.0608(2)	−0.0543(2)
N(4)	0.2095(3)	0.1758(2)	−0.0146(2)
C(1)	0.4307(4)	−0.0492(3)	0.2208(2)
C(2)	0.3569(5)	0.0201(4)	0.3024(3)
C(3)	0.3005(4)	0.1413(3)	0.2597(2)
C(4)	0.1717(4)	0.0066(3)	−0.1232(2)
C(5)	0.0246(4)	0.0869(3)	−0.1284(2)
C(6)	0.0524(4)	0.1919(3)	−0.0592(2)
C(7)	0.2073(4)	−0.1201(3)	−0.1823(3)
C(8)	−0.0614(5)	0.3103(4)	−0.0358(3)
B(1)	0.3083(5)	0.2521(3)	0.0731(3)

Table 8 Fractional atomic coordinates for complex **3**

Atom	*x*	*y*	*z*
Ni	0.0	0.0	0.0
N(1)	0.2025(3)	−0.0114(1)	−0.1052(3)
N(2)	0.2570(3)	0.0488(1)	−0.1864(3)
N(3)	0.0928(3)	0.0909(1)	0.0895(3)
N(4)	0.1514(3)	0.1442(1)	−0.0082(3)
C(1)	0.3151(4)	−0.0683(2)	−0.1164(4)
C(2)	0.4436(4)	−0.0446(2)	−0.2060(4)
C(3)	0.4048(4)	0.0291(2)	−0.2482(4)
C(4)	0.2958(4)	−0.1438(2)	−0.0410(4)
C(5)	0.5002(5)	0.0825(2)	−0.3452(5)
C(6)	0.1146(3)	0.1184(2)	0.2350(4)
C(7)	0.1857(4)	0.1902(2)	0.2307(4)
C(8)	0.2093(4)	0.2053(2)	0.0765(4)
C(9)	0.0671(4)	0.0740(2)	0.3724(4)
C(10)	0.2804(5)	0.2735(2)	0.0033(5)
B(1)	0.1508(5)	0.1237(2)	−0.1837(4)

Table 9 Fractional atomic coordinates for complex **5**

Atom	*x*	*y*	*z*
Co	0.0	0.088 75(5)	−0.25
N(1)	−0.065 8(4)	0.137 5(2)	−0.161 5(1)
N(2)	0.037 5(4)	0.131 5(2)	−0.108 3(1)
N(3)	0.176 9(3)	0.007 6(2)	−0.217 3(1)
N(4)	0.245 3(4)	0.023 3(2)	−0.155 4(1)
C(1)	−0.211 5(5)	0.152 8(3)	−0.136 7(2)
C(2)	−0.198 7(6)	0.157 4(3)	−0.068 0(2)
C(3)	−0.040 2(6)	0.143 5(3)	−0.051 3(2)
C(4)	−0.355 1(5)	0.161 5(3)	−0.180 2(2)
C(5)	0.035 8(7)	0.139 9(5)	0.016 6(2)
C(6)	0.234 7(5)	−0.072 9(3)	−0.239 9(2)
C(7)	0.338 4(5)	−0.109 3(3)	−0.192 5(2)
C(8)	0.343 5(5)	−0.047 6(3)	−0.140 4(2)
C(9)	0.184 9(6)	−0.110 0(3)	−0.307 0(2)
C(10)	0.439 9(6)	−0.051 6(4)	−0.077 2(2)
B(1)	0.216 8(6)	0.118 9(4)	−0.122 0(2)

References

1 H. Irving and R. J. P. Williams, *J. Chem. Soc.*, 1953, 3192.
2 H. Sigel and D. B. McCormick, *Acc. Chem. Res.*, 1970, **3**, 201.
3 J. E. Huheey, E. A. Keiter and R. L. Keiter, *Inorganic Chemistry*, 4th edn., Harper Collins College Publishers, New York, 1993.
4 J. Stary, *The Solvent Extraction of Metal Chelates*, Pergamon, Oxford, 1964.
5 (*a*) N. Yasuda, H. Kokusen, Y. Sohrin, S. Kihara and M. Matsui, *Bull. Chem. Soc. Jpn.*, 1992, **65**, 781; (*b*) Y. Sohrin, H. Kokusen, S. Kihara, M. Matsui, Y. Kushi and M. Shiro, *J. Am. Chem. Soc.*, 1993, **115**, 4128; (*c*) Y. Sohrin, M. Matsui, Y. Hata, H. Hasegawa and H. Kokusen, *Inorg. Chem.*, 1994, **33**, 4376; (*d*) H. Kokusen, Y. Sohrin, H. Hasegawa, S. Kihara and M. Matsui, *Bull. Chem. Soc. Jpn.*, 1995, **68**, 172.
6 S. Trofimenko, *J. Am. Chem. Soc.*, 1967, **89**, 3170; 6288.
7 E. Frauendorfer and G. Agrifoglio, *Inorg. Chem.*, 1982, **21**, 4122.
8 (*a*) J. P. Jesson, S. Trofimenko and D. R. Eaton, *J. Am. Chem. Soc.*, 1967, **89**, 3148; (*b*) S. Trofimenko, *Chem. Rev.*, 1993, **93**, 943.
9 H. M. Echols and D. Dennis, *Acta Crystallogr., Sect. B*, 1976, **32**, 1627.
10 C. K. Johnson, ORTEP, Report ORNL-5138, Oak Ridge National Laboratory, Oak Ridge, TN, 1976.
11 L. J. Guggenberger, C. T. Prewitt, P. Meakin, S. Trofimenko and J. P. Jesson, *Inorg. Chem.*, 1973, **12**, 508.
12 J. R. Jezorek and W. H. McCurdy, jun., *Inorg. Chem.*, 1975, **14**, 1939.
13 R. D. Shannon, *Acta Crystallogr., Sect. A*, 1976, **32**, 751.
14 A. Bondi, *J. Phys. Chem.*, 1964, **68**, 441.
15 M. Eigen, W. Kruse, G. Maass and L. Demaeyer, *Prog. React. Kinet.*, 1964, **2**, 287.
16 N. Walker and D. Stuart, *Acta Crystallogr., Sect. A*, 1983, **39**, 158.
17 G. M. Sheldrick, in *Crystallographic Computing 3*, eds. G. M. Sheldrick, C. Kruger and R. Goddard, Oxford University Press, Oxford, 1985, pp. 175–189.
18 P. T. Beurskens, G. Admiraal, G. Beurskens, W. P. Bosman, S. Garcia-Granda, R. O. Gould, J. M. M. Smits and C. Smykalla, the DIRDIF program system, Technical Report of the Crystallography Laboratory, University of Nijmegen, 1992.
19 TEXSAN, Structure analysis package, Molecular Structure Corporation, Houston, TX, 1985.

Received 28*th April* 1995; *Paper* 5/02711J